Macromolecules
ARTICLE
pubs.acs.org/Macromolecules

Synthesis of Binary Polymer Brushes via Two-Step Reverse Atom Transfer Radical Polymerization

Penglin Ye, Hongchen Dong, Mingjiang Zhong, and Krzysztof Matyjaszewski*

Center for Macromolecular Engineering, Department of Chemistry, Carnegie Mellon University, 4400 Fifth Avenue, Pittsburgh, Pennsylvania 15213, United States

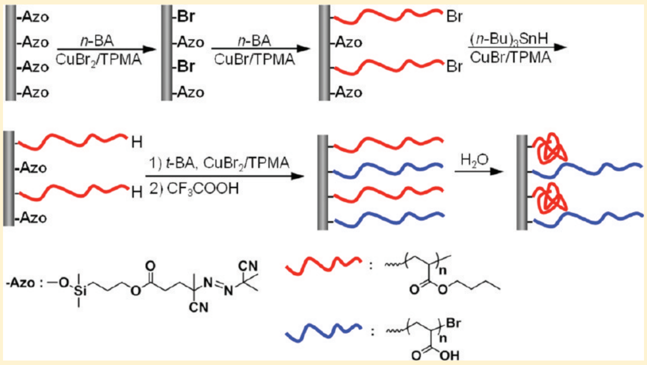

ABSTRACT: Well-defined poly(*n*-butyl acrylate) (P*n*BA)/poly(acrylic acid) (PAA) binary brushes grafted from silicon surfaces have been successfully prepared via a two-step reverse atom transfer radical polymerization (reverse ATRP) of *n*-butyl acrylate and *tert*-butyl acrylate initiated from tethered diazo groups and subsequent hydrolysis of poly(*tert*-butyl acrylate) (P*t*BA). The final molar ratio of P*n*BA/PAA brushes was well-controlled by limiting the time allowed for the initial decomposition of a fraction of the diazo-initiator at higher temperature. After initiating growth of polymer chains from the surface-tethered initiator and deactivation by the Cu(II) complex, ATRP was carried out at 40 °C to achieve desired molecular weight while preventing further decomposition of the remaining unreacted diazo-initiator from which the P*t*BA brushes were grown in the second step. Measurement of film thickness, contact angle, and surface morphology of the resulting surfaces confirmed the P*n*BA/PAA binary brush structures and demonstrated how surface properties changed with composition. The morphologies of the surfaces were affected by treatment with a selective solvent, such as water or toluene, and a nonselective solvent, chloroform/methanol (1:1 by volume).

■ INTRODUCTION

Binary polymer brushes are composed of two different polymer chains immobilized on the surface of a solid substrate. On the basis of the unique properties of each brush, the surfaces show different morphologies and properties and provide the possibility of reversible switching as a result of external signal. The signal is derived from changes in the materials' environment, such as temperature, chemical composition, applied mechanical force, light, or electrical and magnetic field.[1−4]

Binary brushes are conventionally prepared via the "grafting to" approach. For instance, Minko et al. reported sequential grafting of carboxyl-terminated polystyrene (PS) and poly(2-vinylpyridine) (PVP) onto silicon wafers.[5] Tsukruk reported grafting Y-shaped molecules, which have two incompatible polymer chains, PS and poly(*t*-butyl acrylate) (P*t*BA), onto a silicon surface.[6−8] Stamm et al. reported the synthesis of binary polymer brushes, PS/PVP brushes, by a "grafting from" method using a two-step free radical polymerization process.[9] Zhao et al. reported a "grafting from" method utilizing an asymmetric Y-shaped difunctional initiator attached to silicon surfaces.[10−13] The dual functionalities on the Y-shaped initiators immobilized on the substrate surface allowed sequential activation of atom transfer radical polymerization (ATRP) and nitroxide-mediated radical polymerization (NMP) initiators to prepare well-mixed polymer brushes. Recently, a combination of "grafting to" and "grafting from" techniques was reported to provide another route to binary brushes.[14,15]

ATRP is one of the most robust and efficient controlled/living radical polymerizations procedures, yielding well-defined (co) polymers with precisely controlled topology, composition, and functionality.[16−20] A number of methods have been developed for the initiation of an ATRP reaction, including reverse ATRP,[16,21,22] simultaneous reverse and normal initiation (SR&NI),[22,23] activators generated by electron transfer (AGET),[24,25] initiators for continuous activator regeneration (ICAR),[26] and activators regenerated by electron transfer (ARGET).[26−28] In a reverse ATRP, a conventional radical initiator, such as 2,2′-azobis(isobutyronitrile) (AIBN), generates initiating radicals or propagating radicals, $I^\bullet$ or $I{-}P_1^\bullet$, which rapidly react with an oxidized transition-metal species to form a dormant species and the lower oxidation state transition-metal complex. The reaction then proceeds in exactly the same manner as a normal ATRP.[21,22,29]

It is difficult to prepare binary brushes using normal ATRP due to fast and efficient initiation of all tethered (pseudo)halide initiating groups. However, the rate of decomposition of a tethered diazo compound, suitable for initiating a reverse ATRP, is dependent on time and temperature. This article introduces a new method to prepare binary polymer brushes using surface-initiated two-step reverse ATRP. Therefore, the chemical composition and grafting density of the polymer brushes can be controlled through temperature and time of decomposition, enabling the tethered initiator required for the sequential

Received: December 15, 2010
Revised: January 28, 2011
Published: March 02, 2011

"grafting from" reactions via reverse ATRP. A series of well-defined P*n*BA/PAA binary brushes with varied compositions were successfully prepared by grafting from silicon wafers using two-step reverse ATRP. The morphological changes of the tethered binary brushes were characterized via atomic force microscopy (AFM) before and after treatment with different solvents.

■ EXPERIMENTAL SECTION

Materials. Tris[(2-pyridyl)methyl]amine (TPMA) was purchased from ATRP Solutions and used as received. 2,2′-Azobis(isobutyronitrile) (AIBN, 98%) purchased from Aldrich was recrystallized from methanol and stored in a refrigerator prior to use. *N,N,N′,N′′,N′′*-Pentamethyldiethylenetriamine (PMDETA), 2,2,6,6-tetramethylpiperidine-1-oxyl (TEMPO), ethyl 2-bromoisobutyrate (EBiB), and copper(II) bromide were purchased from Aldrich and used as received. *n*-Butyl acrylate (*n*BA, 99%) and *tert*-butyl acrylate (*t*BA, 98%) were purchased from Aldrich and purified by passing through a column filled with basic alumina to remove the inhibitor. The diazo-initiator and surface attachment were synthesized and conducted according to the previously published procedures.[30]

Analyses. Number- and weight-average molecular weight (M_n and M_w, respectively) and M_w/M_n of P*n*BA and P*t*BA were determined by gel permeation chromatography (GPC). GPC was conducted with a Waters 515 pump and Waters 410 differential refractometer using PSS columns (Styrogel 10^2, 10^3, 10^5 Å) in tetrahydrofuran (THF) as an eluent at a flow rate of 1 mL/min at 35 °C. The column system was calibrated with linear polystyrene standards. Conversions were determined by gas chromatography (GC) using a Shimadzu GC-14A gas chromatograph equipped with a FID detector and a ValcoBond 30 m VB WAX Megabore column. The thicknesses of the grafted brushes were obtained by a discrete wavelength ellipsometer PhE-101 (Micro Photonics Inc.) with a He−Ne laser ($\lambda = 632.8$ nm) at a 70° incidence angle. The error of the measurement was less than 0.5 nm. The grafting density (σ) was calculated using the following equation: $\sigma = N_A h\rho/M_w$, where M_w is the weight-average molecular weight, N_A is Avogadro's number, and $\rho = 1.0$ g/cm^3 is the bulk polymer density.

Scheme 1. Synthesis of Binary Brushes via Reverse ATRP

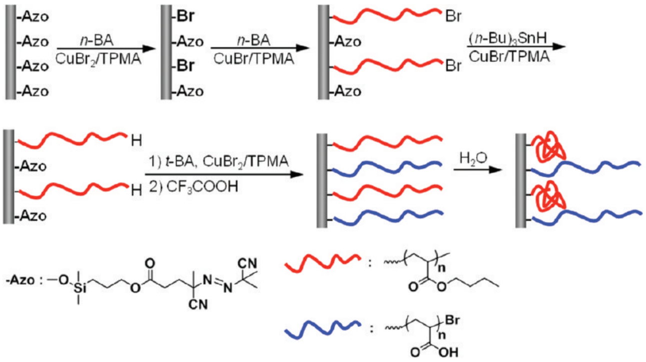

Contact angles were obtained with a VCA Optima contact angle measuring instrument (AST Products, Inc.) with a drop size 1.0 μL of deionized water. Three measurements were made on each surface, and the average contact angle is presented in cf. Table 2. Surface morphology of binary brushes on glass surfaces was analyzed by atomic force microscopy (AFM). Tapping mode AFM experiments were carried out using a Multimode Nanoscope V system (Veeco Instruments). The measurements were performed in air using commercial Si cantilevers with a nominal spring constant and resonance frequency respectively equal to 50−80 N/m and 300 kHz.

Syntheses. *Synthesis of Poly(n-butyl acrylate) (PnBA) via Two-Step Reverse ATRP (Figure 1).* 2,2′-Azobis(isobutyronitrile) (AIBN, 14.4 mg, 87.6 μmol), copper(II) bromide (19.6 mg, 87.6 μmol), tris[(2-pyridyl)methyl]amine (TPMA, 25.4 mg, 87.6 μmol), butyl acrylate (5 mL, 35.0 mmol), and 5.0 mL of *N,N*-dimethylformamide (DMF) were added to a clean dry Schlenk flask. After the solution became homogeneous, the flask was sealed with a glass stopper and then deoxygenated by four freeze−pump−thaw cycles before it was immersed in a thermostated oil bath at 80 °C. After 70 min, the flask was moved to a thermostated oil bath at 40 °C. After 20 h, 2,2,6,6-tetramethylpiperidine-1-oxyl (TEMPO, 10.9 mg, 70.1 μmol) was added. After 2 h, the flask was immersed in a thermostated oil bath at 100 °C for 30 min and then moved to thermostated oil bath at 40 °C. The polymerization was stopped at 78.5 h by opening the flask and exposing the catalyst to air. Samples were taken at timed intervals and analyzed to determine the conversions of *n*BA by GC and the molecular weight by GPC.

Synthesis of PnBA Brushes from Silicon Wafer (Surface 1, Table 1). A silicon wafer modified with diazo-initiator, AIBN (28.8 mg, 175.2 μmol), copper(II) bromide (19.6 mg, 87.6 μmol), TPMA (25.4 mg, 87.6 μmol), *n*-butyl acrylate (5 mL, 35.0 mmol), and 5.0 mL of DMF were added to a clean dry Schlenk flask. After the solution became homogeneous, the flask was sealed with a glass stopper and then deoxygenated by four freeze−pump−thaw cycles before it was immersed in a thermostated oil bath at 80 °C. After 29 min, the flask was moved to a thermostated oil bath at 40 °C. Samples were taken at timed intervals and analyzed by GC to determine the conversions of *n*BA. The polymerization was stopped at 48 h by opening the flask and exposing the catalyst to air. In order to remove the free polymer physically adsorbed onto the surface, the resulting silicon wafer was washed 10 times with methylene chloride. Surfaces 2 and 3 were prepared with a similar method.

Dehalogenation of PnBA Brushes[13,31]. The silicon wafers grafted with P*n*BA brushes, anisole (10 mL), PMDETA (64.5 μL, 0.31 mmol), and EBiB (45 μL, 0.31 mmol) were added to a clean dry Schlenk flask. The flask was sealed with a glass stopper and then deoxygenated by four freeze−pump−thaw cycles. During the final cycle, the flask was filled with nitrogen and CuBr (44.2 mg, 0.31 mmol) was added to the frozen mixture. The flask was sealed with a glass stopper and then evacuated and backfilled with nitrogen four times before it was immersed in a thermostated oil bath at 40 °C. Tri(*n*-butyl)tin hydride (0.25 mL, 0.93

Table 1. Reaction Conditions and Properties of Binary Brushes with Varied Compositions[a]

surface no.	reaction time at 80 °C[b] (min)	M_n (P*n*BA)[c]	M_w/M_n (P*n*BA)[c]	thickness (P*n*BA)[d] (nm)	grafting density (P*n*BA) (chain/nm^2)	M_n (P*t*BA)[c]	M_w/M_n (P*t*BA)[c]	total thickness[d] (nm)	total grafting density (chain/nm^2)
1	29	42 230	1.09	0.96	0.014	39 490	1.23	4.78	0.072
2	70	41 180	1.07	2.69	0.039	41 670	1.13	4.26	0.062
3	163	41 970	1.14	4.54	0.065	42 840	1.04	5.05	0.072

[a] $[nBA]_0$:$[AIBN]_0$:$[CuBr_2]_0$:$[TPMA]_0$ = 400:*X*:1:1 in DMF, where *X* = 2, 1.2, and 0.75 for surfaces 1, 2, and 3, respectively. $[nBA]_0 = 3.50$ M. $[tBA]_0$:$[AIBN]_0$:$[CuBr_2]_0$:$[TPMA]_0$ = 500:0.5:1:1 in DMF. $[tBA]_0 = 2.33$ M. Reverse ATRP of *t*BA was carried out at 100 °C for 30 min to fully decompose AIBN initiator and then at 40 °C until appropriate molecular weight was achieved. [b] Reverse ATRP of *n*BA was carried out at 80 °C for a certain time as listed and then at 40 °C until appropriate molecular weight was achieved. [c] Determined by GPC in THF, based on polystyrene standards. [d] Measured by the ellipsometry.

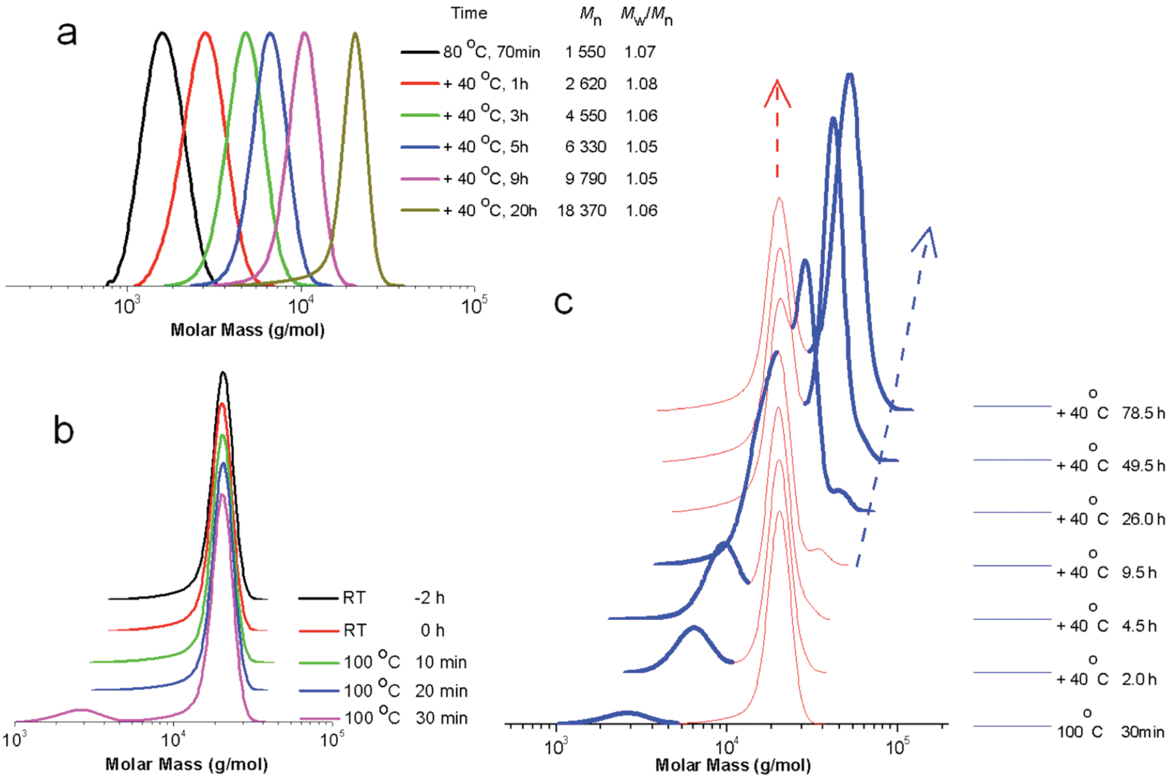

Figure 1. GPC traces of two-step reverse ATRP of *n*BA. (a) $[nBA]_0$:$[AIBN]_0$:$[CuBr_2]_0$:$[TPMA]_0$ = 400:1:1:1 in DMF. The reaction was carried out at 80 °C for 70 min and then conducted at 40 °C. (b) TEMPO was added to the reaction mixture, and the temperature was increased to 100 °C. $[TEMPO]_0$:$[AIBN]_0$ = 0.8:1. (c) After it was heated to 100 °C for 30 min to fully decompose all the remaining AIBN, the reaction solution was conducted at 40 °C until the appropriate molecular weight was achieved.

mmol) was injected via a microsyringe into the mixture over a period of 15 min. The reaction was continued for 1 h. Then the resulting silicon wafer was cleaned with methylene chloride 10 times.

Synthesis of Poly(tert-butyl acrylate) (PtBA) Brushes from Silicon Wafer (Surface 1, Table 1). The silicon wafer with a fraction of unreacted diazo-initiator and tethered P*n*BA brushes, AIBN (6.9 mg, 42.0 μmol), copper(II) bromide (18.8 mg, 84.0 μmol), TPMA (24.4 mg, 84.0 μmol), *t*BA (6 mL, 42.0 mmol), and 6 mL of DMF were added to a clean dry Schlenk flask. After the solution became homogeneous, the flask was sealed with a glass stopper and then deoxygenated by four freeze—pump—thaw cycles before it was immersed in a thermostated oil bath at 100 °C. After 30 min, the flask was moved to a thermostated oil bath at 40 °C. Samples were taken at timed intervals and analyzed by GC to determine the conversions of *t*BA. The polymerization was stopped at 28.5 h by opening the flask and exposing the catalyst to air. In order to remove the free polymer physically adsorbed onto the surface, the resulting silicon wafer was washed with methylene chloride 10 times. Surfaces 2 and 3 were prepared with a similar method.

Hydrolysis of PtBA. The surfaces modified with P*n*BA/P*t*BA brushes were immersed in a mixture of trifluoroacetic acid and tetrahydrofuran (70:30 vol) for 48 h at room temperature. The resulting silicon wafer was cleaned with methylene chloride 10 times.

■ RESULTS AND DISCUSSION

Model Reactions of Two-Step Reverse ATRP. Model reactions of two-step reverse ATRP of *n*BA in DMF initiated from AIBN were first investigated to demonstrate the ability to control the reverse ATRP of *n*BA, subsequent elimination of chain-end functionality, and then reinitiation of the second polymer chain from residual AIBN. The first reaction was conducted at 80 °C for a designated short time to decompose a certain fraction of the added AIBN. Then, the "standard" ATRP reaction was carried out at 40 °C until the desired molecular weight was achieved. This procedure allowed chain growth via ATRP while essentially no AIBN molecules would be decomposed at such a low temperature. Figure 1 shows the gel permeation chromatography (GPC) traces of the polymers formed in the different steps of the model reactions. Figure 1a illustrates ATRP of *n*BA initiated by the fraction of AIBN that was decomposed at 80 °C. The GPC traces are symmetrical and smoothly shifted to higher molecular weight region as the reaction time increases. The molecular weight distribution was narrow, $M_w/M_n < 1.1$. While successful elimination of the bromide chain-end functionality with $(n\text{-Bu})_3SnH$ has been previously reported,[13,31] in the model reaction, 2,2,6,6-tetramethylpiperidin-1-oxyl (TEMPO) was used to replace the bromide atom from the active chain ends.[32] In Figure 1b, the GPC trace 2 h after TEMPO was added to the reaction solution was identical to that before the TEMPO addition, indicating that TEMPO trapped the growing radicals and prevented the further polymerization. After the temperature was increased to 100 °C, there were no changes in the GPC traces during first 10 and 20 min (Figure 1b). This shows the P*n*BA with TEMPO at the chain end did not reinitiate the polymerization at 100 °C. After 30 min, excess TEMPO was completely consumed, and the decomposed remaining AIBN participated in the second step reverse ATRP. It initiated new polymer chains, corresponding to the new peak at low molecular weight in the GPC trace in Figure 1c. The ATRP was then conducted at 40 °C until the appropriate molecular weight was achieved. Figure 1c shows that there are two types of polymer chains in solution: one from the first step which is marked in red and the other one marked in blue. The red GPC traces, which represent the polymer chains formed in the first step, are essentially identical without shifting on molecular weight scale. The blue GPC traces, which correspond to the new polymer chains, continuously shift to high molecular weight as the reaction time increases. This clearly demonstrates that binary polymer chains can be achieved with this conceptual two-step reverse ATRP method.

Table 2. Water Contact Angles of the Grafted Binary P*n*BA/PAA Brushes from Surfaces after $CHCl_3$/MeOH (1:1 by Volume, Nonselective Solvent) and Water Treatment

surface no.	$CHCl_3$/MeOH treatment (deg)	water treatment (deg)
1	72 ± 1	68 ± 1
2	82 ± 1	79 ± 1
3	89 ± 1	86 ± 1

Synthesis of P*n*BA and Poly(acrylic acid) (PAA) Binary Brushes from Silicon Wafer. After validation of the concept of

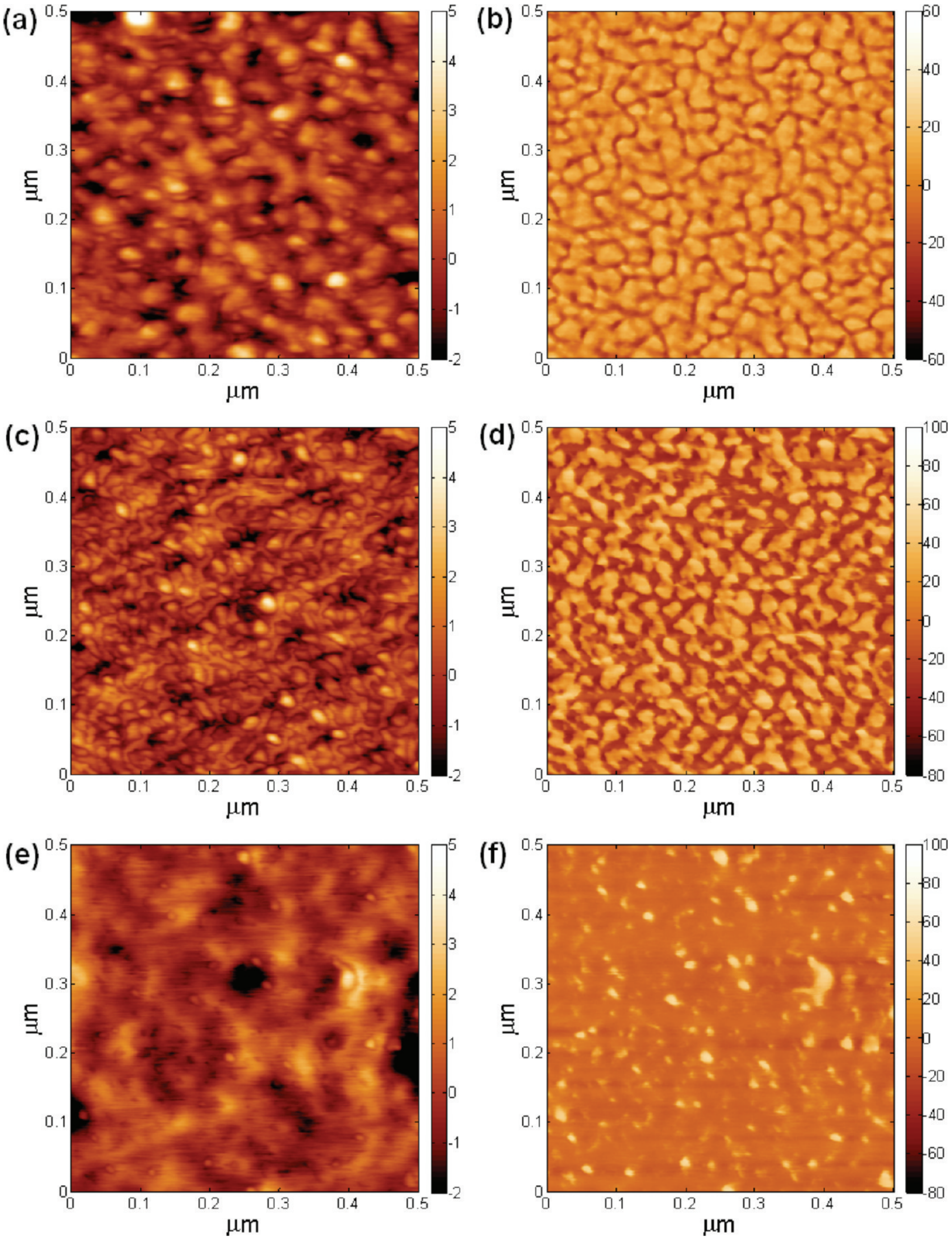

Figure 2. AFM topographical (left) and phase (right) images of the grafted binary P*n*BA/PAA brushes from surfaces 1 (a, b), 2 (c, d), and 3 (e, f) after water treatment.

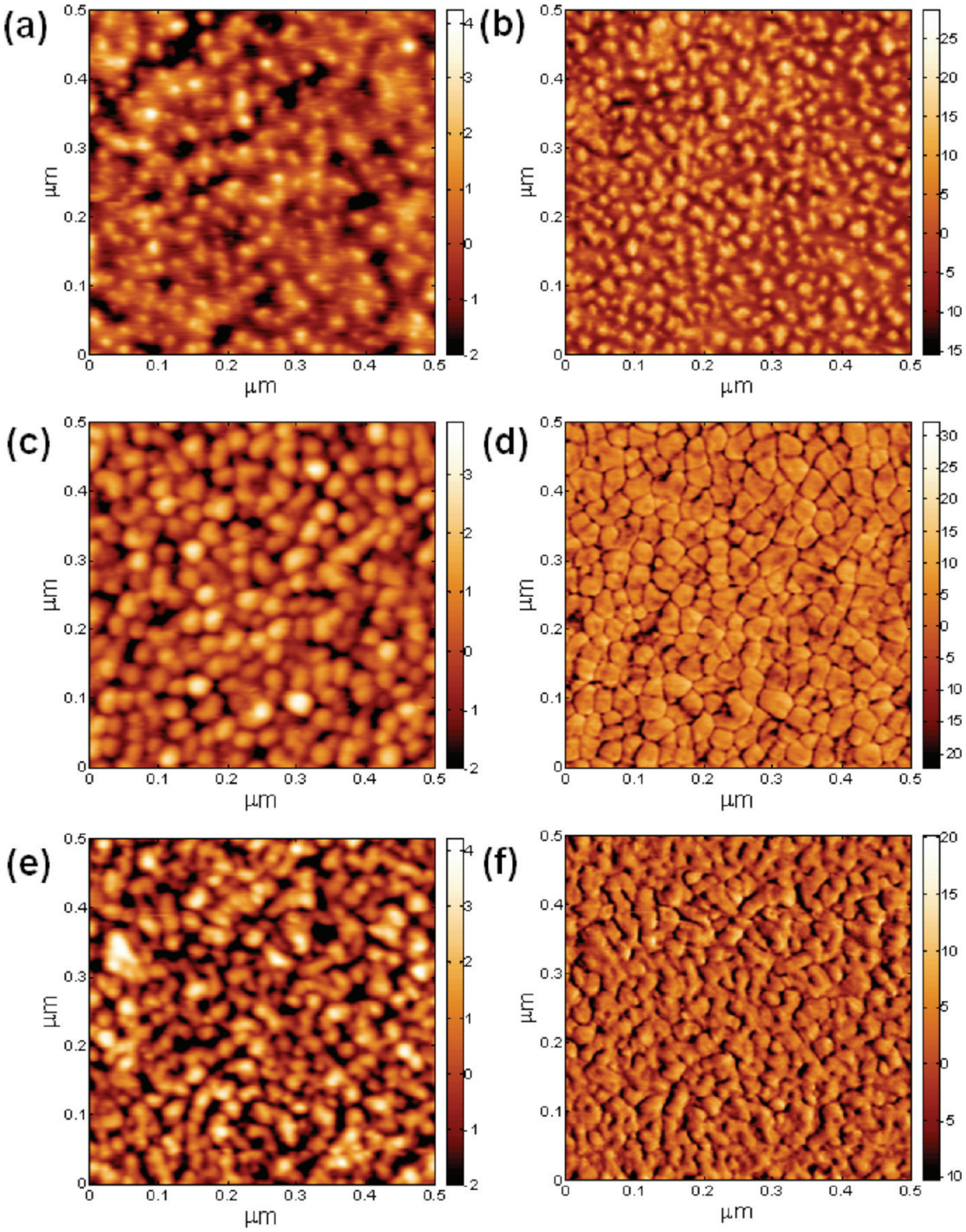

Figure 3. AFM topographical (left) and phase (right) image of the grafted binary brushes from surfaces 1 (a, b), 2 (c, d), and 3 (e, f) after the treatment of toluene.

two-step reverse ATRP, silicon wafers modified with a monolayer of an diazo-initiator were prepared according to procedures reported in the literature.[30] The polymerizations were conducted under the reaction conditions listed in Table 1. Unattached diazo-initiator, AIBN, was added to the reaction medium to simplify evaluation of M_n and M_w/M_n of the tethered polymer brushes, assuming a close correlation between the growth of the free polymer and attached polymer.[33] Through controlling the decomposition time of the tethered diazo-initiator at 80 °C for 29, 70, and 163 min, the grafting density of P*n*BA brushes was 0.014, 0.039, and 0.065 chain/nm^2, respectively (surfaces 1−3 in Table 1). Before initiating the growth of the second P*t*BA brushes, the bromo chain ends of the grafted P*n*BA brushes were removed by reaction with tributyltin hydride to prevent chain extension.[13] Reverse ATRP of *t*BA was then carried out at 100 °C for 30 min to fully decompose all remaining unreacted diazo-initiators on the surface and then continued at 40 °C until the appropriate molecular weight was achieved. After the polymerization of *t*BA, the thickness of polymer layers grafted from all three surfaces increased, compared to the surfaces tethered only with P*n*BA brushes. The grafting density of the final binary brushes increased from 0.014, 0.039, and 0.065 to 0.06 and 0.07 chain/nm^2, indicating that P*t*BA brushes were successfully grafted from the remaining surface tethered diazo-initiators. The relatively low

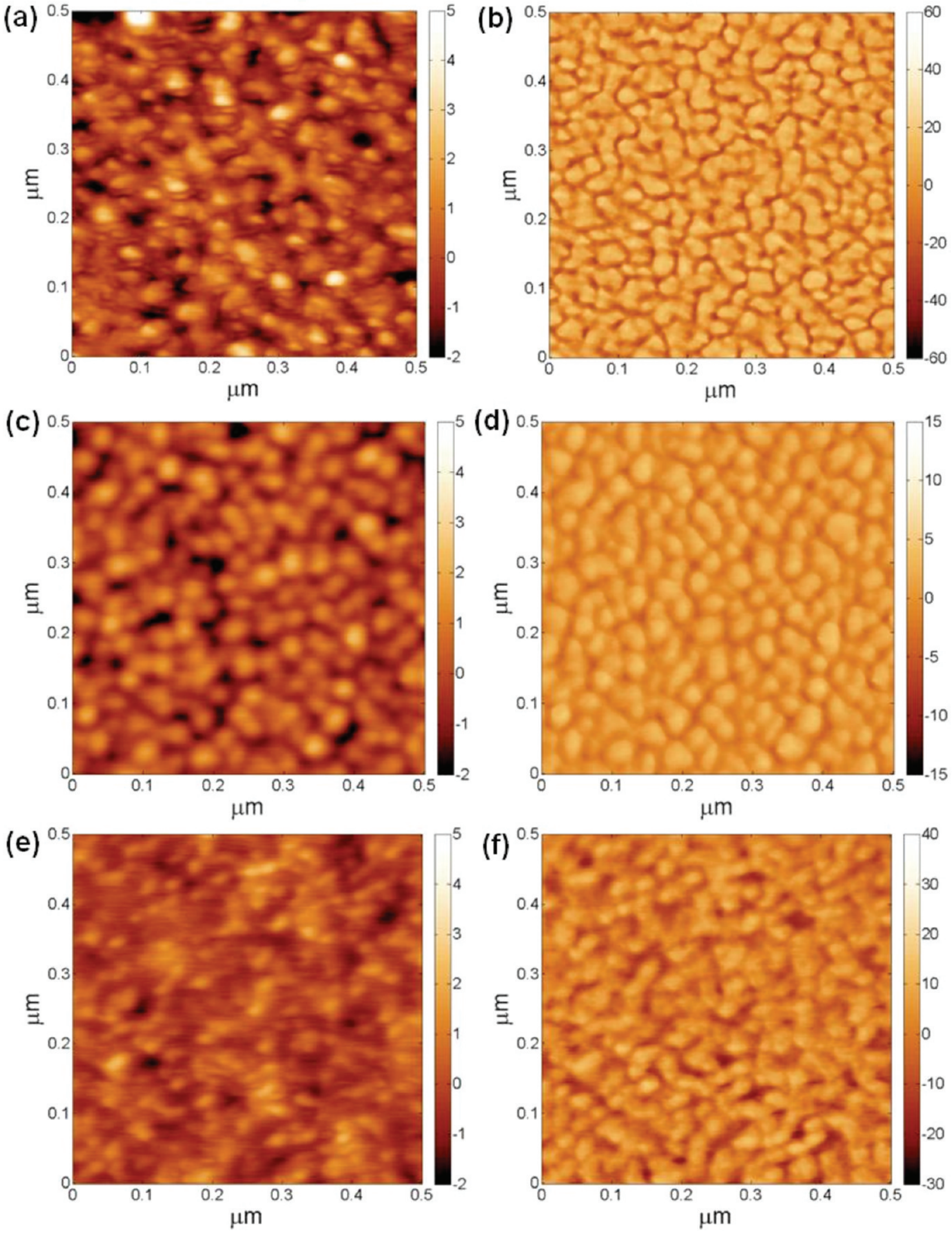

Figure 4. AFM topographical (left) and phase (right) image of the grafted binary brushes from surfaces 1 (a, b), 2 (c, d), and 3 (e, f) after the treatment of a nonselective solvent (chloroform/methanol = 1:1 by volume).

grafting density may be caused by the low efficiency with which decomposed diazo molecules initiate polymer chains surrounded by existing polymer brushes. Finally, all the surfaces were treated with trifluoroacetic acid to convert the P*t*BA to PAA.

Solvent-Responsive Surface Morphology of P*n*BA/PAA Binary Brushes. The water contact angle of P*n*BA/PAA binary brushes was measured after treatment with different solvents. The results in Table 2 show that after treatment with a nonselective solvent, $CHCl_3$/MeOH (1:1 by volume), the surfaces became more hydrophobic than those treated with water due to an increase in the surface density of P*n*BA chains. The lowest water contact angle, 72°, was observed for surface 1, which has the highest ratio of PAA to P*n*BA, about 9:1. After treatment with water, the water contact angle of the surfaces decreased because PAA brushes stretched out while the P*n*BA brushes collapsed near to the surface.

Figures 2, 3, and 4 show AFM topographical and phase images of the grafted binary P*n*BA/PAA brushes from surfaces 1 to 3 after water, chloroform/methanol, and toluene treatments. The images clearly demonstrate that P*n*BA and PAA brushes segregate due to dissimilar chemical properties. The P*n*BA/PAA binary brushes displayed switchable properties and changed surface morphology

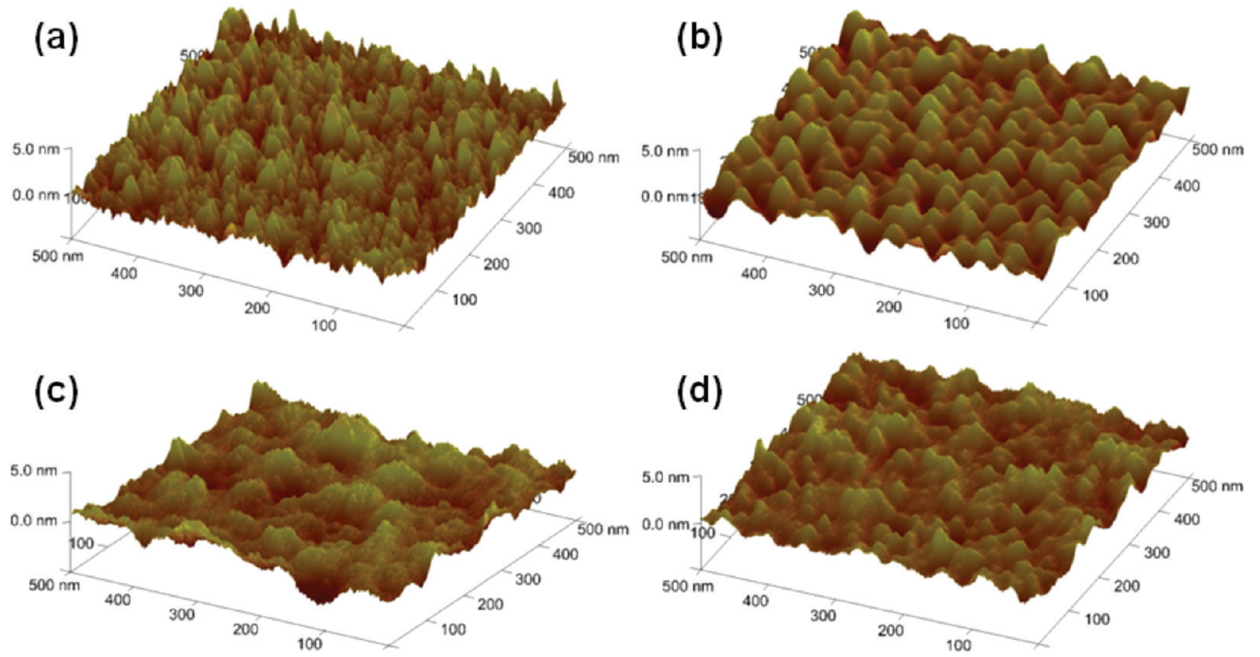

Figure 5. 3D AFM topographical images of the grafted binary P*n*BA/PAA brushes from surfaces 2 (a, b) and 3 (c, d) after the treatments of water (a, c) and a nonselective solvent (chloroform/methanol = 1:1 by volume) (b, d).

when treated with different solvents. Water is a better solvent for PAA than for P*n*BA brushes; only PAA brushes chains extend upon water treatment. The lateral dimensions of PAA domains, shown as bright parts in the phase images in Figure 2, decrease from above 40 nm to about 10 nm while the density of P*n*BA brushes increased from 0.014 to 0.065 chain/nm^2. Moreover, the coverage of PAA domains is significantly decreased from surface 1 to surface 3. Toluene is a better solvent for P*n*BA than PAA brushes; therefore, P*n*BA brushes chain instead of PAA brushes extend upon toluene treatment. Figure 3 shows the lateral dimensions of P*n*BA domains increases in size from about 20 nm to above 50 nm while the density of P*n*BA brushes increases from 0.014 to 0.065 chain/nm^2. The coverage of P*n*BA domains is significantly increased from surface 1 to surface 3. For the same surface, the change in domain size clearly shows the switchable properties with water and toluene treatment.

Chloroform/methanol (1:1 by volume) is a nonselective solvent, good for both P*n*BA and PAA brushes. The domains of the binary brushes became connected, and the variation in the height of the domains gradually decreased due to structural rearrangement of the surface (Figure 4). The 3D height images of surfaces 2 and 3 after treatment with water and chloroform/methanol (1:1 by volume) also show the change of morphology for the P*n*BA/PAA binary brushes (Figure 5). The roughness of surfaces 2 and 3 decrease from 0.61 to 0.57 nm and from 0.61 to 0.47 nm, respectively, after water and chloroform/methanol (1:1 by volume) treatment. The scale of the measured area is 500 nm × 500 nm.

CONCLUSION

We demonstrate the successful preparation of well-defined P*n*BA/PAA binary brushes, with different ratios of the two brushes, via a two-step reverse ATRP of *n*BA and *t*BA and subsequent hydrolysis of P*t*BA. The grafting density of the first P*n*BA brush was controlled by varying the time the reaction medium was exposed to decomposition of the diazo initiator at high temperature. ATRP of *n*BA was then carried out at 40 °C for a sufficient time to achieve the desired molecular weight while preventing further decomposition of the remaining diazo-initiator from which P*t*BA brushes were grown in the second step. It was observed that the thickness of the polymer layer increased after the growth of the second stage P*t*BA brushes. The water contact angle and surface morphology of P*n*BA/PAA brushes were different for the different compositions and exhibited switchable changes upon treatment with a selective solvent or a nonselective solvent. This two-step reverse surface-initiated ATRP can be extended to prepare multicomponent mixed brushes based on the wide range of monomers polymerizable by ATRP and reverse ATRP. This method can therefore be extended to styrenes, (meth) acrylates, (meth)acrylamides, acrylonitrile, and other monomers. Compared to the traditional grafting-onto method, this grafting-from approach is able to generate more uniformly distributed binary brushes without formation of large domains due to physical property difference. Compared to normal surface-initiated ATRP, the two-step reverse surface-initiated ATRP resulted in relatively low grafting density due to termination of immobilized diazo-initiators. The grafting density could be increased by lowing the temperature of the initiation stage or using more active Cu(II)/ligand catalyst to decrease the concentration of radical generated from diazo-initiators. The investigation of reverse ATRP from silica nanoparticles is in progress in order to understand more about the kinetics of this new approach.

AUTHOR INFORMATION

Corresponding Author

*E-mail: km3b@andrew.cmu.edu.

ACKNOWLEDGMENT

The authors thank the National Science Foundation (DMR 09-69301) WCU (World Class University) program through the

Korea Science and Engineering Foundation funded by the Ministry of Education, Science and Technology (R33-10035-0) and members of the CRP Consortium at Carnegie Mellon University for their financial support. We gratefully acknowledge contribution of Dr. Fabio Paris for the help of synthesis of the diazo-initiator.

■ REFERENCES

(1) Luzinov, I.; Minko, S.; Tsukruk, V. V. *Prog. Polym. Sci.* **2004**, *29* (7), 635–698.

(2) Luzinov, I.; Minko, S.; Tsukruk, V. V. *Soft Matter* **2008**, *4* (4), 714–725.

(3) Zhao, B.; Zhu, L. *Macromolecules* **2009**, *42* (24), 9369–9383.

(4) Stuart, M. A. C.; Huck, W. T. S.; Genzer, J.; Mueller, M.; Ober, C.; Stamm, M.; Sukhorukov, G. B.; Szleifer, I.; Tsukruk, V. V.; Urban, M.; Winnik, F.; Zauscher, S.; Luzinov, I.; Minko, S. *Nature Mater.* **2010**, *9* (2), 101–113.

(5) Draper, J.; Luzinov, I.; Minko, S.; Tokarev, I.; Stamm, M. *Langmuir* **2004**, *20* (10), 4064–4075.

(6) Julthongpiput, D.; Lin, Y.-H.; Teng, J.; Zubarev, E. R.; Tsukruk, V. V. *Langmuir* **2003**, *19* (19), 7832–7836.

(7) Julthongpiput, D.; Lin, Y.-H.; Teng, J.; Zubarev, E. R.; Tsukruk, V. V. *J. Am. Chem. Soc.* **2003**, *125* (51), 15912–15921.

(8) Lin, Y.-H.; Teng, J.; Zubarev, E. R.; Shulha, H.; Tsukruk, V. V. *Nano Lett.* **2005**, *5* (3), 491–495.

(9) Sidorenko, A.; Minko, S.; Schenk-Meuser, K.; Duschner, H.; Stamm, M. *Langmuir* **1999**, *15* (24), 8349–8355.

(10) Zhao, B.; He, T. *Macromolecules* **2003**, *36* (23), 8599–8602.

(11) Zhao, B.; Haasch, R. T.; MacLaren, S. *Polymer* **2004**, *45* (23), 7979–7988.

(12) Zhao, B.; Haasch, R. T.; MacLaren, S. *J. Am. Chem. Soc.* **2004**, *126* (19), 6124–6134.

(13) Li, D.; Sheng, X.; Zhao, B. *J. Am. Chem. Soc.* **2005**, *127* (17), 6248–6256.

(14) Berger, S.; Synytska, A.; Ionov, L.; Eichhorn, K.-J.; Stamm, M. *Macromolecules* **2008**, *41* (24), 9669–9676.

(15) Zhang, Y.; He, H.; Gao, C. *Macromolecules* **2008**, *41* (24), 9581–9594.

(16) Wang, J.-S.; Matyjaszewski, K. *J. Am. Chem. Soc.* **1995**, *117* (20), 5614–15.

(17) Matyjaszewski, K.; Miller, P. J.; Shukla, N.; Immaraporn, B.; Gelman, A.; Luokala, B. B.; Siclovan, T. M.; Kickelbick, G.; Vallant, T.; Hoffmann, H.; Pakula, T. *Macromolecules* **1999**, *32* (26), 8716–8724.

(18) Matyjaszewski, K.; Xia, J. *Chem. Rev.* **2001**, *101* (9), 2921–2990.

(19) Braunecker, W. A.; Matyjaszewski, K. *Prog. Polym. Sci.* **2007**, *32* (1), 93–146.

(20) Matyjaszewski, K.; Tsarevsky, N. V. *Nature Chem.* **2009**, *1* (4), 276–288.

(21) Xia, J.; Matyjaszewski, K. *Macromolecules* **1999**, *32* (16), 5199–5202.

(22) Qiu, J.; Pintauer, T.; Gaynor, S. G.; Matyjaszewski, K.; Charleux, B.; Vairon, J.-P. *Macromolecules* **2000**, *33* (20), 7310–7320.

(23) (a) Gromada, J.; Matyjaszewski, K. *Macromolecules* **2001**, *34* (22), 7664–7671. (b) di Lena, F.; Matyjaszewski, K. *Prog. Polym. Sci.* **2010**, *35* (8), 959–1021.

(24) Jakubowski, W.; Matyjaszewski, K. *Macromolecules* **2005**, *38* (10), 4139–4146.

(25) Min, K.; Gao, H.; Matyjaszewski, K. *J. Am. Chem. Soc.* **2005**, *127* (11), 3825–30.

(26) Matyjaszewski, K.; Jakubowski, W.; Min, K.; Tang, W.; Huang, J.; Braunecker, W. A.; Tsarevsky, N. V. *Proc. Natl. Acad. Sci. U.S.A.* **2006**, *103* (42), 15309–15314.

(27) Jakubowski, W.; Matyjaszewski, K. *Angew. Chem., Int. Ed.* **2006**, *45* (27), 4482–4486.

(28) Jakubowski, W.; Min, K.; Matyjaszewski, K. *Macromolecules* **2006**, *39* (1), 39–45.

(29) Xia, J.; Matyjaszewski, K. *Macromolecules* **1997**, *30* (25), 7692–7696.

(30) Prucker, O.; Ruehe, J. *Macromolecules* **1998**, *31* (3), 592–601.

(31) Coessens, V.; Matyjaszewski, K. *Macromol. Rapid Commun.* **1999**, *20* (2), 66–70.

(32) Matyjaszewski, K.; Woodworth, B. E.; Zhang, X.; Gaynor, S. G.; Metzner, Z. *Macromolecules* **1998**, *31* (17), 5955–5957.

(33) Tsujii, Y.; Ohno, K.; Yamamoto, S.; Goto, A.; Fukuda, T. Structure and Properties of High-Density Polymer Brushes Prepared by Surface-Initiated Living Radical Polymerization. In *Surface-Initiated Polymerization I*; Springer: Berlin, 2006; Vol. 197, pp 1−45.